



Numerical modeling and sensitivity analysis of seawater intrusion in a dual-permeability coastal karst aquifer with

5 conduit networks

Zexuan Xu^{1,*}, Bill X. Hu² and Ming Ye³

10 ¹Climate and Ecosystem Sciences Division, Lawrence Berkeley National Laboratory,
Berkeley, California, 94720, USA

²Institute of Groundwater and Earth Sciences, Jinan University, Guangzhou, Guangdong,
China

³Department of Scientific Computing, Florida State University, Tallahassee, Florida,
15 32306, USA

*Corresponding author: email address: xuzexuan@gmail.com;

Submitted to Hydrology and Earth System Sciences



Abstract

In a coastal karst aquifer, seawater intrudes significantly landward through the highly permeable subsurface conduit system, and contaminates the groundwater resources in the porous medium. In this study, a two-dimensional coupled density-dependent flow and transport SEAWAT model is developed to study seawater intrusion in the dual-permeability karst aquifer. To provide guideline for modeling seawater intrusion in such an aquifer, local and global sensitivity analysis are conducted to evaluate the parameters of boundary conditions and hydrological characteristics, including hydraulic conductivity, effective porosity, specific storage and dispersivity of the conduit and the porous medium. In the local sensitivity analysis, simulations are more sensitive to all parameters at the seawater and freshwater mixing zone than elsewhere. The most important parameter for simulations in both domains is salinity at the submarine spring, which is also the boundary condition of the conduit. The hydrological characteristics of the conduit network are not only important to the simulations in the conduit, but also significantly affect the simulations in the porous medium, due to the interactions between the two systems. Therefore, salinity and head observations in the conduits and karst features have more values for calibrating the models and understanding seawater intrusion in a coastal karst aquifer. Compared to the local sensitivity analysis, the global sensitivity results are different in several parameters (hydraulic conductivity, porosity and the boundary conditions at the submarine spring), mainly due to the non-linear relationship of the parameters with respect to the simulations. The results of global sensitivity analysis also indicate that the Darcy's equation does not accurately calculate the conduit flow rate with hydraulic conductivity



in the continuum SEAWAT model. Dispersivity is no longer an important parameter in
45 the advection-dominated transport aquifer system with conduit, compared to the
sensitivity results in a homogeneous porous medium. Based on the sensitivity analysis,
the extents of seawater intrusion are quantitatively evaluated with the identified important
parameters, including salinity at the submarine spring with rainfall recharge, sea level rise
and longer simulation time under an extended low rainfall period.

50

Key Words: Seawater intrusion; Coastal karst aquifer; Variable-density numerical model;
Dual-permeability karst system; Sensitivity analysis

1. Introduction

55 Many serious environmental issues have been caused by seawater intrusion in the
coastal regions, such as soil salinization, marine and estuarine ecological changes, and
groundwater contamination (Bear, 1999). Groundwater salinization is the primary
detrimental effect of seawater intrusion to groundwater resources, since mixing with less
than 1% of seawater (250 mg/L chloride) by volume makes freshwater non-potable
60 (WHO, 2011). Custodio (1987) and Shoemaker (2004) summarized the controlling
factors of seawater intrusion into a coastal aquifer, including the geologic and lithological
heterogeneity, localized surface recharge, paleo-hydrogeological conditions and
anthropogenic influences. Werner et al. (2013) concluded that climate variations,
groundwater pumping, and fluctuating sea levels are important to the mixing of seawater
65 and freshwater. On the other hand, sea level rise has been recognized as a serious
environmental threat in this century (Voss and Souza, 1987; Bear, 1999; IPCC, 2007).



Sea level fluctuation has significant and complex impacts on seawater intrusion in a coastal aquifer under different conditions (Werner et al., 2013). The Ghyben-Herzberg relationship indicates that rising sea level causes extended seawater intrusion in a coastal 70 aquifer, and significantly moves the mixing interface position further landward (Werner and Simmons, 2009). Essink et al. (2010) pointed out that seawater intrusion is exacerbated under sea level rise conditions in a large time scale due to global climate change. Likewise, high tides associated with hurricanes or tropical storms have been found to temporarily affect the extent of seawater intrusion in a coastal aquifer (Moore 75 and Wilson, 2005; Wilson et al., 2011). However, tide fluctuation is generally negligible to mixing interface movement over a regional and large time scale (Inouchi et al., 1990).

Modeling seawater intrusion in a coastal aquifer requires a coupled density-dependent flow and transport numerical model. In such model, the solution of seawater is based on the groundwater velocity field from flow modeling, and salinity in turn 80 determines water density and affects the simulation of flow field. Several variable-density numerical models have been developed and widely used, including SUTRA (Voss and Provost, 1984) and FEFLOW (Diersch, 2002). SEAWAT is a widely used density-dependent model, which solves flow equations by finite difference method, and transport 85 equations by three major classes of numerical techniques (Guo and Langevin, 2002; Langevin et al., 2003). Generally speaking, most variable-density models are numerically complicated and computational expensive, because of the small timestep and the implicit procedure of solving flow and transport equations iteratively many times within each timestep (Werner et al., 2013).



Karst aquifer is particularly vulnerable to groundwater contamination including

90 seawater intrusion in the coastal regions, since the well-developed sinkholes, karst windows, and subsurface conduit networks are highly permeable and usually connected. The caves are found directly open to the sea and become submarine springs below the sea level, connected with the conduit network as natural pathways for seawater intrusion. The highly permeable subsurface conduit network in a coastal karst aquifer cause seawater 95 intrude significantly further landward and contaminate freshwater resources. The preferential flow within the conduit also significantly moves the position of seawater and freshwater mixing zone landward in karst aquifers (Calvache and Pulido-Bosch, 1997). Fleury et al. (2007) reviewed a number of studies about freshwater discharge and seawater intrusion through karst conduits and submarine springs in the coastal karst 100 aquifers, and summarized some important controlling factors, including hydraulic gradient of equivalent freshwater head, hydraulic conductivity, and seasonal precipitation variation. Rainfall and regional freshwater recharges significantly affect the extents of seawater intrusion. Salinity near the outlet of conduit system is diluted by freshwater discharge during a rainfall season, but remains constant as saline water during a low 105 rainfall period (Martin and Dean, 2001; Martin et al., 2012).

The Woodville Karst Plain (WKP) is a typical coastal karst aquifer, where the Spring Creek Springs (SCS) is a first magnitude spring consisting of 14 submarine springs located in the Gulf of Mexico (Fig. 1). SCS is also an outlet of the subsurface conduit network, exactly located at the shoreline beneath the sea level. Tracer test studies 110 and cave diving investigations indicate that the conduit system starts from the submarine spring and extends 18 km landward connecting with an inland spring called Wakulla



Spring, although the exact locations of the subsurface conduits are unknown and difficult to explore (Kernagis et al., 2008; Kincaid and Werner, 2008). Some evidence shows that seawater intrusion has been observed through subsurface conduit system for more than 18
115 km in the WKP (Xu et al., 2016). The relationship of seawater intrusion, groundwater flow and rainfall recharges in the WKP was described by a conceptual model of groundwater flow cycling in Davis and Verdi (2014), and then quantitatively simulated by a CFPv2 model in Xu et al. (2015b). In addition, Davis and Verdi (2014) also point out that sea level rise at the Gulf of Mexico in the past century could be a reason for the
120 increasing discharge at an inland karst spring (Wakulla Spring) and decreasing discharge at SCS, when the hydraulic gradient towards the Gulf between the two springs decreases.

(Insert Fig. 1 here)

Modeling groundwater flow in a dual-permeability karst aquifer is challenging, because of the non-laminar flow calculation in a karst conduit system (Davis, 1996;
125 Shoemaker et al., 2008; Gallegos et al., 2013). Several coupled discrete-continuum numerical models have been developed and applied to solve the non-laminar flow in the conduit and the Darcian flow in a porous medium simultaneously, such as MODFLOW-CFPm1 (Shoemaker et al., 2008) and CFPv2 (Reimann et al., 2014; Reimann et al., 2013;
Xu et al., 2015a; Xu et al., 2015b). However, these models only solve constant density
130 governing equations, which are not applicable for simulating the density-dependent seawater intrusion processes in a coastal aquifer. The VDFST-CFP developed by Xu and Hu (2017) is a density-dependent discrete-continuum modeling approach to study seawater intrusion in a coastal karst aquifer with conduits, however, is only able to simulate synthetic cases but not yet for the field scale applications. Therefore, the



135 variable-density SEAWAT model is still used in this study, in which Darcy equation is
not only used to calculate flow rate in the porous medium, but also the conduit flow rate
with large values of hydraulic conductivity and effective porosity.

Very few studies addressed the parameter sensitivities of seawater intrusion in a
coastal karst aquifer. Shoemaker (2004) performed a sensitivity analysis of the SEAWAT
140 model for seawater intrusion in a homogeneous aquifer with porous medium, and
concluded that dispersivity is an important parameter to the head, salinity and
groundwater flow simulations and observations in transition zone. Shoemaker (2004) also
concluded that salinity observations are more effective than head observation, and the
“toe” of the transition zone is the most effective location for head and salinity simulations
145 and observations. The sensitivity results in this study confirms some conclusions in
Shoemaker (2004), and highlights the significance of conduit network in simulating
seawater intrusion in a coastal karst aquifer, mainly due to the interaction between the
karst conduit and the porous medium.

In this study, the local and global sensitivity analyses are conducted to evaluate
150 the head and salinity simulations with respect to parameters in a coupled density-
dependent flow and transport model. To our knowledge, this is the first attempt to assess
the parameter sensitivities for seawater intrusion in a vulnerable dual-permeability karst
aquifer with conduit network. The rest of the paper is arranged as follows: the details of
local and global sensitivity analysis are introduced in Sect. 2. The model setup,
155 hydrological conditions, model discretization, initial and boundary conditions are
discussed in Sect. 3. The results of local and global sensitivity analysis are discussed in



Sect. 4. The scenarios of seawater intrusion simulation with different boundary conditions and elapsed time are presented in Sect. 5. The conclusions are made in Sect. 6.

160 **2. Methods**

The governing equations solved in the SEAWAT model can be found in the Guo and Langevin (2002), including the variable-density flow equation with additional density terms, and advection dispersion solute transport equation. The local and global sensitivity methods used in this study are briefly introduced below.

165

2.1 Local sensitivity analysis

In this study, UCODE_2005 (Poeter and Hill, 1998) is applied in the local sensitivity analysis, which evaluates the derivatives of model simulations with respect to parameters at the specified values (Hill and Tiedeman, 2006). The forward difference 170 approximation of sensitivity is calculated as the derivative of the i th simulation respect to the j th model parameters,

$$\left. \frac{\partial y'_i}{\partial x_j} \right|_b \approx \frac{y'_i(x + \Delta x) - y'_i(x)}{\Delta x_j} \quad 1)$$

where y'_i is the value of the i th simulation; x_j is the j th estimated parameter; x is a vector of the specified values of estimated parameter; Δx is a vector of zeros except that the j th parameter equals Δx_j .

175 The sensitivities are calculated by running the model once using the parameter values in x to obtain $y'_i(x)$, and then changing the j th parameter value and running the model again in $x + \Delta x$ to obtain $y'_i(x + \Delta x)$. Scaled sensitivities are used to compare the



parameters sensitivities that may have different units. In UCODE_2005, a scaling method is used to calculate the dimensionless scaled sensitivities (DSS) by the following equation,

$$dss_{ij} = \left(\frac{\partial y'_i}{\partial x_j} \right) \Big|_x |x_j| \omega_{ii}^{1/2} \quad 2)$$

180 where dss_{ij} is the dimensionless scaled sensitivity of the i th simulation with respect to the j th parameter; ω_{ii} is the weight of the i th simulation.

The DSS values of different simulations with respect to each parameter are accumulated as the composite scaled sensitivities (CSS). The CSS of the j th parameter is evaluated via:

$$css_j = \sum_{i=1}^{ND} \left[(dss_{ij})^2 \Big|_x / ND \right]^{1/2} \quad 3)$$

185 where ND is the number of simulated quantities, for example, the head and salinity simulations in this study.

2.2 Morris method in global sensitivity analysis

The local sensitivity analysis is conceptually straightforward and easy to compute without expensive computational cost. However, the sensitivity indices for parameters are calculated at the specified values only, but not for the entire parameter ranges. In addition, the indices are approximated in the first order derivative only, assuming a linear relationship of simulated quantities with respect to parameters. The higher orders relationship and interactions among parameters are not considered in the local sensitivity analysis.



The global sensitivity analysis evaluates the simulations with respect to parameters within the entire parameter range, instead of the specified values in the local sensitivity analysis. Morris method is applied to evaluate the global parameter sensitivities in this study (Morris, 1991). It is a so-called “one-step-at-a-time” method (OAT), meaning that 200 only one input parameter is perturbed and given a new value in each run. The Morris method is made by a number r of local changes at different points of the possible range of input values. In each parameter, a discrete number of values called levels are chosen with the parameter ranges of variation. Two sensitivity measures are proposed by Morris method for each parameter: the mean μ that estimates the overall effect of the factor on 205 the output, and the standard deviation σ that estimates the ensemble of the second or higher-order effects (Saltelli et al., 2004). The mean μ and standard deviation σ of the EEs are evaluated with the r independent random paths in the Morris method,

$$\mu = \sum_{i=1}^r d_i / r \quad 4)$$

$$\sigma = \sqrt{\sum_{i=1}^r (d_i - \mu)^2 / r} \quad 5)$$

The k -dimensional vector x of the model parameters has components x_i , which can 210 be divided into p uniform intervals. The effect of changing one parameter at a time is evaluated in turn by the elementary effect (EE), d_i , which is defined as,

$$d_i = \frac{1}{\tau_y} \frac{[y(x_1^*, \dots, x_{i-1}^*, x_i^* + \Delta, x_{i+1}^*, \dots, x_k^*) - y(x_1^*, \dots, x_k^*)]}{\Delta} \quad 6)$$



where Δ is the relative distance in the coordinate; τ_y is the output scaling factor; $\{x_i^*\}$ is the parameter set selected by different sampling method.

To compute the EE for the k parameters, $(k+1)$ simulations are needed in the same
215 way as local sensitivity method for the perturbation of each parameter, which is called
one “path” (Saltelli et al., 2004). An ensemble of EEs for each parameter is generated by
multiple paths of randomly generated parameter set. The total number of calculation is
 $r(k+1)$ when Monte Carlo random sampling is applied, where r is the number of paths.

However, the global sensitivity analysis of this study does not apply Monte Carlo
220 random sampling, which needs extremely large numbers (>250) of paths to be generated
for 11 parameters. The program takes very long time to complete the random sampling
and sensitivity computation without parallelization. To save the running time and
computational cost but obtain reliable result, the trajectory sampling is developed by
Saltelli et al. (2004) and becomes a widely-used method to generate the ensembles of EEs
225 for Morris method in the global sensitivity analysis. The definition of p -level is the same
as Monte Carlo sampling, where $\Delta = \pm p/[2(p-1)]$, either positive or negative. The
trajectory method starts by randomly selecting a “base” value x^* for the vector x . Each
component x_i of x^* is sampled from the set $(0, 1/(p-1), 2/(p-1), \dots, 1)$. The randomly
selected vector x^* is used to generate the other sampling points but not one of them,
230 which means that the model is never evaluated at vector x^* . The first sampling point, $x^{(1)}$,
is obtained by changing one or more components of x^* by Δ . The choice of components
 x^* to be increased or decreased is conditioned by that $x^{(1)}$ still being within the domain.
The second sampling point, $x^{(2)}$, is generated from x^* with the property that it differs



from $x^{(1)}$ in its i th component, which has been either increased or decreased by Δ , but
235 also still being within the domain. The third sampling point, $x^{(3)}$, differs from $x^{(2)}$ for
only one component j , for any $j \neq i$, will be $x_j^{(3)} = x_j^{(2)} + \Delta$. A succession of $(k+1)$
sampling points $x^{(1)}, x^{(2)}, \dots, x^{(k+1)}$ is produced in the input parameters space called a
trajectory, with the key characteristic that two consecutive points differ in only one
component. As a result, any component i of the ‘base’ vector x^* has been selected at least
240 once by Δ in order to calculate one EE for each parameter.

Once a trajectory is constructed and evaluated by Morris method, an EE for each
parameter i , $i = 1, \dots, k$, can be computed. If $x^{(l)}$ and $x^{(l+1)}$, with l in the set in $(1, \dots, k)$,
are two sampling points differing in their i th component, the EEs associated with the
parameter i is,

$$d_i(x^{(l)}) = \frac{[y(x^{(l+1)}) - y(x^{(l)})]}{\Delta}, \quad 7)$$

245 A random sample of r EEs is selected at the beginning of sampling. Each
trajectory sampling has a different starting point that is randomly generated. The points
belonging to the same trajectory are not independent, but the r points sampled from each
distribution belonging to different trajectories are independent.

3. Model development

250 In this study, a two-dimensional SEAWAT model is setup to simulate seawater
intrusion through the major subsurface conduit network in the Woodville Karst Plain
(WKP) (Fig. 1). Figure 2 presents a schematic figure of the cross section in a coastal karst
aquifer with a conduit network and a submarine spring opening to the sea. The model
spatial domain is not a straight line from the submarine Spring Creek Springs to Wakulla



255 Spring, but a cross section along the major conduit pathway of seawater intrusion in the coastal karst aquifer. The model spatial domain and geometry in this study is setup exactly as the regional scale in the field, for example, the 18 km long and 91 meters deep conduit network in the WKP.

(Insert Fig. 2 here)

260 However, this study only addresses the seawater intrusion through the conduit, and the flow and solute exchanges between the conduit and the surrounding porous medium within the cross section. In the field, seawater intrudes further landward through the conduit network and flows into the surrounding porous medium, in both the vertical and the horizontal direction that perpendicular to the cross section. The simulation of 265 saltwater flow and transport in the perpendicular direction within the porous medium is beyond the scope of the model used in this study, which only aims to study seawater intrusion through the conduit and the porous medium of the cross section. This assumption of 2D model is reasonable, considering that the exchange fluxes from the conduit to the surrounding porous medium trivially affect the seawater intrusion through 270 the channel, when the conduit wall exchange permeability is relatively smaller compared with the large permeability in the conduit. The simplified model is used in this study, since the main purpose of this study is to evaluate the role of subsurface conduit in seawater intrusion in the coastal karst aquifer. In addition, most SEAWAT models are setup for 2D cross section with high-resolution vertical discretization. 3D coupled 275 density-dependent flow and transport model is rarely seen, due to the constraint of computational cost. The parameter sensitivities of 3D density-dependent numerical model are even more difficult to be evaluated within a reasonable time frame, because running



the model many times with parameters perturbation are required in the sensitivities analysis.

280

3.1 Hydrological conditions

Table 1 presents the hydrological characteristics of the Upper Floridan Aquifer (UFA) in the WKP. The parameter values are evaluated in the following local sensitivity analysis and applied in the seawater intrusion scenarios in Sect. 5. These parameters have 285 been calibrated in the regional-scale groundwater flow and solute transport models by Davis et al. (2010), and have been applied in many previous modeling studies (Gallegos et al., 2013; Xu et al., 2015a; Xu et al., 2015b). This study does not aim to re-calibrate the model, since observation data in the field are insufficient, especially in the subsurface conduit. The head and salinity measurements in the conduit are rarely available, due to 290 the difficulties of subsurface conduit investigation and monitoring devices installation.

(Insert Table 1 here)

The hydrological characteristics (hydraulic conductivity, specific storage and effective porosity) of the conduit system are generally greater than the surrounding porous medium. Hydraulic conductivity of the porous medium is assigned as 2286 m/day 295 (7500 ft/day), and as large as 610,000 m/day (2,000,000 ft/day) for the conduit system. Even the hydraulic conductivity of porous medium in the study region is larger than most alluvial aquifers, because of the numerous small fractures and relatively large pores in a karst aquifer due to dissolution of carbonate rocks. Specific storage and effective porosity in the porous medium are assumed as 5×10^{-7} and 0.003, respectively. Specific storage 300 and effective porosity are 0.005 and 0.300 in the conduit layer, respectively. The



longitudinal dispersivity is estimated as 10 m in the porous medium, but is assumed very small (0.3 m) in the conduit, because advection is dominated and dispersion is negligible in the solution of transport in the conduit.

305 **3.2 Spatial and temporal discretization**

The grid discretization and boundary conditions of the two-dimensional SEAWAT numerical model are shown in Fig. 3, which consists of 140 columns and 37 layers in the cross section. Guo and Langevin (2002); Werner et al. (2013) pointed out that higher-resolution grid discretization in the vertical direction is required for modeling 310 the density-dependent flow. The vertical thickness of each cell is set uniformly as 3.048 m (10 ft) in this study, with significantly higher resolution than the 152 m (500 ft) thickness in many previous constant-density modeling studies in the WKP, for example, Davis and Katz (2007); Davis et al. (2010); Xu et al. (2015a); Gallegos et al. (2013); Xu et al. (2015b).

315 (Insert Fig. 3 here)

The horizontal dimension for each cell is set uniformly 152 m (500 ft) as the scales in the field, except columns #22 and #139, which are 15.2 m (50 ft) as the vertical conduit network connecting the submarine spring (SCS) and inland spring (Wakulla Spring), respectively. The sizes of spring outlets and the conduit are based on the 320 observations data in the field and the calibrated models in previous studies (Gallegos et al., 2013). However, the diameter of horizontal conduit network is assumed homogeneous in this study. The outlet of vertical conduit system is the submarine spring (SCS) located at the shoreline at column #22. The conduit system starts from the



submarine spring, descends downward to layer #29 (nearly 100 m below sea level),
325 horizontally extends nearly 18 km from column #22 to column #139, and then rises
upward to the top through column #139. Seawater intrudes at the SCS on the first layer of
column #22, and then flows vertically downward into the conduit system. The inland
spring is simulated by the DRAIN package as general head boundary condition in the
SEAWAT model. All layers are simulated as confined aquifer since the conduit is fully
330 saturated, which are identical to the previous numerical models used in Davis et al.
(2010); Xu et al. (2015a); Xu et al. (2015b) in the WKP.

In this study, a transient 7-day stress is simulated in the SEAWAT model. The
scenarios of longer simulation time are exceptions for evaluating seawater intrusion
under an extended low rainfall period in Sect. 5.4. The timestep of flow model is set as
335 0.1 days, and the timestep of transport model is determined by SEAWAT automatically.

3.3 Initial and boundary conditions

The initial condition of head is set 0.0 m as the present-day sea level for the cells
from the left boundary to the shoreline (column #22), and gradually rises to 1.52 m (5.0
340 ft) at inland boundary on the right, based on the elevation of the inland spring. Please
note that values of head are written in the input files of SEAWAT model, instead of
equivalent freshwater head. The initial conditions of salinity are assumed constant along
the vertical direction in each column. Salinity at the leftmost 10 columns is set uniformly
as 35.0 PSU (Practical Salinity Unit) as seawater without mixing near the sea boundary.
345 The seawater/freshwater mixing zone has the salinity initial condition from 35 PSU at
column #11 to 0 PSU at column #45, with a gradient of 1.0 PSU per column. Salinity is



set uniformly as 0.0 PSU from column #46 to the inland boundary on the right, as uncontaminated freshwater before seawater intrudes. Several testing cases have been made to test and confirm that the initial conditions trivially affect the modeling results.

350 The boundary conditions are also presented in Fig. 3. The bottom of model domain is no-flow boundary condition as the less-permeable confining unit of the UFA base. The constant head and concentration inland boundary condition on the right is 1.5 m (5.0 ft) as the elevation of inland spring, and 0.0 PSU as uncontaminated freshwater. The seawater boundary on the left is 3.38 km away from the shoreline, set as 0.0 m
355 constant head as the present-day sea level and 35.0 PSU constant concentration as seawater without mixing. However, the boundary conditions of head and salinity at the submarine spring (column #22, layer #1) are adjusted and evaluated in the scenarios of different sea level, salinity and rainfall conditions in Sect. 5.

360 **4. Sensitivity Analysis**

Sensitivity analysis evaluates the uncertainties of salinity and head simulations with respect to eleven parameters, provides the knowledge for understanding the hydrological characteristics and boundary conditions in a coastal karst aquifer with a conduit. The symbols and definitions of the eleven parameters in the SEWAT model are listed in Table 1, as well as the specified evaluated values in local sensitivity analysis, and the parameter ranges in the global sensitivity analysis (Table 1). There are six parameters in the groundwater flow model, including hydraulic conductivity (HY_P and HY_C), specific storage (SS_P and SS_C) of the conduit and the porous medium, recharge rate (RCH) and the sea level at the submarine spring (H_SL). The other five



370 parameters, including effective porosity (PO_P and PO_C), dispersivity (DISP_P and
DISP_C) of the conduit and the porous medium, and the salinity at the submarine spring
(SC), are in the solute transport model.

4.1 Local sensitivity analysis

375 In the local sensitivity analysis, the CSS (composited scaled sensitivities) of
parameters with respect to head and salinity simulations are calculated at several
locations in the conduit and the porous medium domains. Again, the specified parameter
values in the local sensitivity analysis are consistent with the hydrological characteristics
of the UFA, and the head and salinity boundary conditions of the conduit outlet are set as
380 present-day sea level and seawater without mixing. The simulation results with the
parameters in the local sensitivity analysis are presented in Sect. 5.1, as the maximum
seawater intrusion case. Parameter sensitivities are computed at several locations, from
column #25 to column #75 with an interval of 5 cells along the horizontal conduit (layer
#29), where column #25 is very close to the shoreline and column #75 is basically the
385 uncontaminated freshwater aquifer. The parameter sensitivities of simulations in a porous
medium are evaluated at layer #24, 15.2 m (50 ft) or 5 layers above the conduit layer,
from column #25 to column #75 with an interval of 5 cells along the horizontal direction.

4.1.1 Local sensitivity analysis of simulations in the conduit

390 Figure 4 shows the arithmetic mean of CSS for each parameter with respect to
simulations in all evaluated locations along the conduit layer. The largest CSS value in
the local sensitivity analysis indicates that salinity at the submarine spring (SC) is the



most important parameter to both salinity and head simulations. Hydraulic conductivity, specific storage and effective porosity of the conduit (HY_C, SS_C and PO_C) as well as
395 sea level at the submarine spring (H_SL) are also important parameters. Hydraulic conductivity, specific storage and effective porosity of the porous medium (HY_P, SS_P and PO_P), recharge rate (RCH) and dispersivity (DISP_C and DISP_P) are the less important parameters. Generally speaking, the parameter sensitivities with respect to head simulations are similar and consistent with salinity simulations.

400 (Insert Fig. 4 here)

Salinity at the submarine spring (SC) is the most important parameter, because the submarine spring is the boundary condition and the major source of seawater intrusion through the conduit network in a coastal karst aquifer. Seawater enters the conduit system at the submarine spring, and continuously intrudes landward through the subsurface conduit system. Seawater also flows into the surrounding porous medium via the exchanges between the two domains, when the equivalent freshwater head in the conduit is larger than the surrounding porous medium. Increasing salinity at the submarine spring causes further seawater intrusion through the conduit network with higher equivalent freshwater head, moves the mixing zone position further landward, and vice versa. The
410 salinity at the submarine spring is determined by freshwater mixing and dilution from the conduit network, in other words, is controlled by the rainfall recharges and freshwater discharge from the aquifer to the sea. In other word, freshwater dilution is represented by salinity at submarine study instead of the recharge flux on the boundary, which is unknown and difficult to quantitatively estimate in a two-dimensional numerical model
415 In addition, the simulations in the conduit are more sensitive to hydraulic conductivity,



specific storage and effective porosity of the conduit (HY_C, SS_C and PO_C) rather than the hydrological characteristics of the porous medium (HY_P, SS_P and PO_P), since conduit network is the major pathway for seawater intrusion. The sea level at the submarine spring (H_SL) is indicated as an important boundary condition in the model,

420 but is not as important as the salinity at the submarine spring (SC). In other words, the extent of seawater intrusion in the conduit is more sensitive to rainfall recharge and freshwater discharge that represented by the parameter SC, rather than the sea level and/or tide level variations. Recharge (RCH) is not an important parameter with respect to simulation in this study, which only represents a small portion of total rainfall recharge

425 in the two-dimensional seawater intrusion model, since the rainfall recharges in the whole springshed converge into the subsurface conduit. In this study, salinity at the submarine spring represents the rainfall recharge with the largest CSS value, instead of the parameter RCH.

In the local sensitivity analysis, the conduit and porous medium dispersivities

430 (DISP_C and DISP_P) are not important to salinity and head simulations, because advection is dominated in the transport of seawater within the highly permeable conduit network, while dispersion is negligible in such rapid flow condition. This is different from the results of parameter sensitivities in a homogeneous aquifer, where dispersivity is actually a very important parameter. Meanwhile, the dispersion solution and dispersivity

435 sensitivities are hardly calculated when conduit flow becomes turbulent. On the other hand, the numerical dispersion is significantly greater than the solution of dispersion equation in the conduit. The Peclet number can be as great as 2500, which is obviously beyond the Peclet number criteria (<4) for solving the advection dispersion transport



equation by finite difference method. In other words, the calculation of salinity dispersion
440 is inaccurate in the conduit by the SEAWAT model with large uncertainty, which brings
about the inaccurate results of dispersivity sensitivities .

Six parameters with the largest CSS are presented in Fig. 5, with respect to the
combination of head and salinity simulations in the evaluated locations along the conduit
network, from column #25 to column #75. The largest CSS values for all parameters are
445 found at either column #50 or #55 within the conduit, matches the position of
seawater/freshwater mixing zone along the conduit network in the maximum seawater
intrusion case in Sect. 5.1. The CSS values are relatively larger for all parameters at the
mixing zone, because head and salinity simulations only change significantly near the
mixing zone but remain constant in other locations.

450 (Insert Fig. 5 here)

4.1.2 Local sensitivity analysis of simulations in the porous medium

Figure 6 shows the arithmetic mean of CSS for each parameter with respect to
head and salinity simulations in all evaluated locations along the porous medium (layer
455 #24). Similar to the parameter sensitivities of simulations in the conduit, the largest CSS
indicates that salinity at the submarine spring (SC) is still the most important parameter
with respect to simulations in the porous medium, although it is a boundary condition of
the conduit system. However, some parameter sensitivities are different from the results
of simulations in the conduit. The hydraulic conductivity and effective porosity of both
460 the conduit and porous medium (HY_C, HY_P, PO_C & PO_P), specific storage of the
conduit (SS_C) and dispersivity of the porous medium (DISP_P) have smaller CSS than



the parameter SC, but are still identified as relatively important parameters. The other parameters (DISP_C, RCH and SS_P) are not important to the simulations in the porous medium. The CSS of the eight relatively important parameters are plot at different evaluated locations along the layer of porous medium in Fig. 7. Similar to the sensitivity analysis of simulations in the conduit, the largest CSS of each parameter is found at either column #35 or #40, matches the mixing zone position in the porous medium in the maximum seawater intrusion case in Sect. 5.1.

(Insert Fig. 6 and 7 here)

465 Salinity at the submarine spring (SC) is still the most important parameter for simulations in the porous medium, because the submarine spring is the major source and the entrance of seawater intrusion into the aquifer. The conduit network is the major pathway for seawater intruding landward and flowing into the surrounding porous medium. Similarly, the conduit hydrological characteristics, such as hydraulic conductivity, effective porosity and specific storage (HY_C, PO_C and SS_C), are also important parameters with respect to the simulations in the porous medium. Groundwater flow and seawater transport through the conduit system have significant impact on the head and salinity simulations in the surrounding porous medium. On the other hand, the hydrological characteristics of porous medium, including hydraulic conductivity, effective porosity and dispersivity (HY_P, PO_P and DISP_P), also have large CSS with respect to simulations in the porous medium. It is easy to understand that head and salinity simulations are sensitive to the in-situ hydrological characteristics of porous medium. In summary, simulations in the porous medium are sensitive to the hydrological characteristics of both the conduit and the porous medium, indicating that the interaction



485 between the two domains are important for simulating seawater intrusion in a dual-permeability coastal karst aquifer. As a result, salinity and head observations in the conduits and other karst features have significant meanings and values for calibrating numerical models and for understanding seawater intrusion in a coastal karst aquifer.

490 **4.2 Global sensitivity analysis**

The derivatives of head and salinity simulations with respect to the selected parameters are calculated to test if the CSS values in the local sensitivity analysis is representative for the entire parameter range (Fig. 8). For example, head and salinity simulations in the conduit are nearly constant to the dispersivity of the porous medium 495 (DISP_P), which is evaluated as an unimportant parameter in the local sensitivity study. Simulation in the porous medium shows a linear relationship to the parameter HY_P, with a median level CSS calculated in the local sensitivity analysis. However, both head and salinity simulations are non-linear to salinity at the submarine spring (SC), which is the most important parameter and the boundary condition of conduit system with the 500 largest CSS (Fig. 8). The local sensitivity analysis is only based on the specified parameter value, but not representative for the entire parameter ranges and higher-order derivatives. Therefore, the global sensitivity analysis is necessary for fully evaluating the relationship of simulations with respect to parameters.

(Insert Fig. 8 here)

505 In the following global sensitivity analysis, parameter sensitivities with respect to simulations are calculated in a specified location in the conduit (column #50, layer 29) and the porous medium (column #35, layer #24), respectively. The parameters



sensitivities have the largest CSS in these locations, which are identical to the mixing zone position is in the maximum seawater intrusion case in Sect. 5.1. The Trajectory
510 sampling method developed by Saltelli et al. (2004) is introduced in Sect. 2.2 and applied in this study, with the recommended choice of $p = 4$ and $r = 10$ by Saltelli et al. (2004).

5.2.1 Global sensitivity analysis to simulations in the conduit

In the global sensitivity analysis, the mean and standard deviation of the EEs for
515 each parameter with respect to salinity simulation in the conduit (column #50, layer #29) are presented in Fig. 9a. The largest mean value indicates that parameter SC is the most important parameter to salinity simulations. It is consistent with the result in local sensitivity analysis, since the submarine spring is the boundary condition of the major pathway for seawater intrusion in the numerical model. The non-linear relationship of
520 salinity simulation with respect to parameter SC shown in Fig.8 is the main reason for the largest standard deviation of the EEs, since the derivatives vary at different evaluated values. Similar to the local sensitivity analysis, the hydraulic conductivity and effective porosity of the conduit (HY_C and PO_C), as well as sea level (H_SL), are all important to salinity simulation with relatively large mean and standard deviation values of EEs.
525 These parameters are either the hydrological characteristics or the boundary conditions of conduit network. However, other parameters are relatively less important with small mean and standard deviation of EEs. Generally speaking, the global sensitivity study results for salinity simulation in the conduit are similar to the local sensitivity analysis.

(Insert Fig. 9 here)



530 The global parameter sensitivities with respect to head simulation exhibit more complicated (Fig. 9b). The mean and standard deviation of EEs for each parameter with respect to head simulation are smaller than the sensitivities of salinity simulation, which means that salinity is more sensitive than head simulation with respect to the parameters. The mean values of EEs indicate that the specific storage (SS_C) and effective porosity
535 (PO_C) of the conduit are the two most important parameters with respect to the head and salinity solutions in the coupled density-dependent flow and transport model, respectively. The values of specific storage and effective porosity are calculated by the percentage of void space in the aquifer, based on the physically measured data in the field. Although salinity at the submarine spring (SC) does not have the largest mean of EEs, it
540 is still an important parameter for head simulation with a large standard deviation of EEs, since the derivatives vary in different evaluated locations, with non-linear relationship to head simulation (Fig. 8). Head simulations are also sensitive to the boundary conditions of salinity in the transport model, because equivalent freshwater head is a function of density in terms of salinity simultaneously in the coupled variable-density flow and
545 transport model.

The means and standard deviations of EEs for effective porosity and specific storage of the conduit (PO_C and SS_C) are much larger than hydraulic conductivity (HY_C), indicating that head simulation in the conduit is more sensitive to effective porosity and specific storage, rather than the hydraulic conductivity. The sensitivity result
550 is different from the common knowledge and empirical experience in hydrogeology, but is actually reasonable in karst modeling. The uncertainty of non-laminar flow rate calculation in the continuum model is highlighted in the sensitivity analysis. In the



SEAWAT model, the Darcy equation estimates the specific discharge in the whole model domain including the conduit system, however, is only accurate for laminar seepage flow
555 in the porous medium. Groundwater flow easily becomes non-laminar and higher than the critical Reynolds number in the conduit system with giant diameter. In such case, the conduit flow rate is non-linear to head gradient and beyond the applicability of Darcy equation, which means that the Darcy equation in SEAWAT model has relatively large error in the non-laminar conduit flow calculation. As a result, the sensitivities of
560 hydraulic conductivity have significant uncertainty to evaluate the permeability of conduit system under non-laminar flow condition.

5.2.2 Global sensitivity analysis of simulations in the porous medium

The means and standard deviations of EEs for each parameter with respect to
565 salinity simulations in the porous medium are shown in Fig. 10a. The mean and standard deviation values indicate that parameters HY_P and SC are the two most important parameters for simulations in the porous medium. Hydraulic conductivity of the porous medium (HY_P) is an important term for solving head and groundwater seepage velocity in the flow equation, which then determines the advective velocity of transport equation
570 in the porous medium. As the boundary condition of conduit system, salinity at the submarine spring (SC) is also important as the major source of seawater intrusion not only in the conduit system, but also in the surrounding porous medium via exchanges between the two domains. The global sensitivity analysis of parameter SC highlights the significance of the interaction between the conduit and the porous medium domains in a
575 dual-permeability aquifer. However, salinity at the submarine spring (SC) with respect to



simulations in the porous medium has the largest CSS in the local sensitivity study, while the CSS of hydraulic conductivity of the porous medium (HY_P) is much smaller (Fig. 6).

Parameter sensitivity of salinity at submarine spring (SC) is evaluated at the specified value (35.0 PSU) with the largest derivative in the local sensitivity analysis (Fig. 8).

580 However, simulations are non-linear to the parameter SC with variable sensitivities. In other words, global sensitivity analysis provides more comprehensive knowledge of parameter sensitivities within the ranges. Sea level at the submarine spring (H_SL) and effective porosity of the porous medium (PO_P) are important parameters to salinity simulations as well. Similar to salinity at the submarine spring (SC), sea level (H_SL) is 585 the boundary condition of flow model in the conduit system, which has great impacts on head and salinity solutions in the surrounding porous medium via exchange between the two domains. The EEs of effective porosity and specific storage of the conduit (PO_C and SS_C) also have relatively large mean and standard deviation to salinity simulation in the porous medium, highlight the values of dynamic interaction between the conduit 590 and the porous medium in this study.

(Insert Fig. 10 here)

On the other hand, the mean and standard deviation of EEs of parameters indicate that the matrix hydraulic conductivity (HY_P) is the most important parameter for head simulation in the porous medium (Fig. 10b), as a common knowledge in groundwater 595 modeling. Please note this is different from the global sensitivity results of simulations in the conduit, in which the EEs of effective porosity and specific storage of the conduit (PO_C and SS_C) have larger mean and standard deviation values than hydraulic conductivity (HY_C), due to the significant uncertainty of conduit flow calculation in the



continuum SEAWAT model. Although not as significant as parameter HY_C, effective
600 porosity of the porous medium (PO_P) is an important parameter with relatively large
mean and standard deviation of EEs, because equivalent freshwater head is calculated by
water density in terms of salinity in the coupled flow and transport model. On the other
hand, sea level at the submarine spring (H_SL) is also an important parameter with
respect to head simulation in the porous medium. As the boundary condition of the
605 conduit, parameter H_SL affects head solutions in the surrounding porous medium by
determining the head-dependent exchange flux between the two domains. In general, the
boundary conditions (SC and H_SL) and hydrological properties (SS_C, HY_C and
PO_C) of the conduit system have great impacts on head simulations in the porous
medium.

610 Both local and global sensitivity analysis highlight that field observations and
numerical simulations of the karst features, including the boundary conditions and
hydrological characteristics of sinkholes, karst windows and subsurface conduit system,
are important to model uncertainty analysis. Simulations in the porous medium are
sensitive to hydrological characteristics and boundary conditions of the conduit,
615 indicating the significance of conduit system on modeling seawater intrusion in a dual-
permeability karst aquifer. The conduit system serves as the major pathway for seawater
intrusion further landward and groundwater contamination in the aquifer. On the other
hand, dispersivity is no longer an important parameter in this study, compared with the
sensitivity analysis in Shoemaker (2004) that dispersivity is found as an important
620 parameter, in which a homogeneous porous medium domain is evaluated without the
preferential advective flow. In a dual-permeability karst aquifer system, advection



transport is dominated in the conduit and the surrounding porous medium as well, while dispersion becomes relatively less important. In this study, the uncertainty of dispersivity sensitivities can be significant, since the large Peclet number in the conduit is beyond its 625 criteria for solving transport equation by finite difference method. An experiment of inactivating DSP package in SEAWAT confirms that the mixing is mostly due to the numerical dispersion instead of the solution of dispersion equation in this study.

In general, parameter sensitivities of simulations in the porous medium are more complicated than those in the conduit, especially for the head simulations. The global 630 sensitivity analysis provides an insight of the parameter interactions and the higher-order relationship with respect to simulations.

5. Seawater Intrusions in Scenarios

Sensitivity analysis finds that salinity at the submarine spring (SC) is the most 635 important parameter with respect to head and salinity simulations in both the conduit and the porous medium. Sea level at the submarine spring (H_SL) is the other important boundary condition of the conduit system in the SEAWAT model. The hydrological conditions of the aquifer are represented by these two boundary conditions, such as rainfall and regional freshwater recharges (SC), and the sea/tide level at the submarine 640 spring (H_SL). In order to evaluate the impacts of boundary conditions on seawater intrusion in a dual-permeability system, the extents of seawater intrusion under scenarios of boundary conditions are simulated by the SEAWAT model and quantitatively measured. In addition, the length of elapsed time in simulation is constant in the sensitivity analysis for consistent comparison purposes. The extents of seawater intrusion



645 in a coastal karst aquifer during an extended low rainfall periods are evaluated by
extending the elapsed time in simulation in Sect. 5.4. In each scenario, only one
parameter is adjusted and others remain the same as the original values in the maximum
seawater intrusion case.

650 **5.1 The maximum seawater intrusion case**

The head and salinity boundary conditions at the submarine spring are set as 0.0
m as the present-day sea level, and 35.0 PSU as seawater without mixing filled in the
conduit system outlet, respectively. In the local sensitivity analysis, parameter
sensitivities are evaluated at the specified parameter values in this case. This case is
655 called the maximum seawater intrusion case, in which the longest distance of seawater
intrusion is simulated by assuming that freshwater dilution by rainfall recharge is
negligible in the entire aquifer, and the outlet of conduit system is filled with seawater
without mixing. Figure 11 presents the salinity and head simulations in the cross section
with a 7-day simulation. This case is also set as the benchmark for the following
660 scenarios.

(Insert Fig. 11 here)

According to the Ghyben-Herzberg relationship, high-density seawater intrudes
landward through the deep aquifer beneath the freshwater flowing seaward on the top.
The equivalent freshwater head at the submarine spring is calculated as 2.29 m (7.5 ft)
665 when salinity is 35.0 PSU at the submarine spring, and seawater without mixing is filled
with the 91 meters deep submarine cave of the conduit. The equivalent freshwater head is
higher than the 1.52 m (5.0 ft) constant head at the inland spring, diverts the hydraulic



gradient landward and causes seawater to intrude into the aquifer. Seawater moves significantly further landward through the highly permeable conduit network, also 670 gradually intrudes landward in the surrounding porous medium via exchange on the conduit wall. The position of seawater/freshwater mixing zone in the deep porous medium beneath the conduit is only slightly behind the seawater front in the conduit, because high-density saline water easily moves downward from the conduit into the deeper aquifer. The area with relatively smaller salinity to the left of the vertical conduit 675 network near the shoreline is due to the freshwater discharge dilution from the aquifer to the sea, since the equivalent freshwater head only increases at the submarine spring but remains constant as 0 m in other areas. Simulation result shows that the mixing zone position in the conduit, defined as the location with salinity of 5.0 PSU, reaches nearly 5.80 km landward from the shoreline. The width of mixing interface, defined as the 680 distance between the locations with salinity of 1.0 PSU and 25.0 PSU, is about 7 grid cells or 1.13 km (0.7 miles) in both the conduit and porous medium.

5.2 Salinity variation at the submarine spring (SC)

Sensitivity analysis indicates that the salinity at the submarine spring (SC) is 685 generally the most important parameter with respect to simulations in both the conduit and the porous medium. In this study, rainfall and regional freshwater recharges are simulated by salinity at the submarine spring instead of time-variable flux on the boundary condition. Salinity at the submarine spring is diluted by large amount of rainfall recharge and freshwater discharge after a significant precipitation event, but remains high 690 after an extended low rainfall period as the maximum seawater intrusion case in Sect. 5.1.



The equivalent freshwater head at the submarine spring is calculated as 2.29 m (7.5 ft) when seawater without mixing is filled with the conduit system, however, proportionally decreases with the salinity at the submarine spring to 0.0 m, when salinity is 0.0 PSU and freshwater is filled with the conduit system. The impact of freshwater recharge on
695 seawater intrusion is evaluated in four scenarios with different salinity at the submarine spring of 0.0 PSU, 10.0 PSU, 20.0 PSU and 30.0 PSU. The head boundary condition is kept constant as 0.0 m as present-day sea level (Fig. 12). The mixing zone positions in both the conduit and porous medium are located at 4.0 (4.5) km away from the shoreline in the cases of salinity of 10.0 (20.0) PSU at the submarine spring. Rainfall recharge and
700 freshwater discharge move the interface significantly seaward. In addition, the mixing zone is very close to the shoreline in the case of salinity of 0.0 PSU at the submarine spring, when seawater intrusion is suspended and blocked by large amount of freshwater dilution. The shape of mixing interface is similar to the maximum seawater intrusion benchmark. However, the width of mixing interface is much wider due to the smaller or
705 even reversed hydraulic gradient from the aquifer to the sea. In such scenarios, the solution of dispersion equation is more important in salinity simulation with slower groundwater seepage flow. Generally speaking, seawater no longer intrudes significantly inland after a heavy rainfall event, and the mixing interface moves seaward when freshwater dilutes the salinity at the submarine spring and the conduit network.
710 (Insert Fig. 12 here)



5.3 Sea level variation at the submarine spring (H_SL)

Sensitivity analysis indicates that sea level at the submarine spring is also an important parameter. Approximate 1.0 m sea level rise at the beginning of next century is predicted by IPCC (2007), with significant impacts on seawater intrusion in a coastal karst aquifer. The extents of seawater intrusion in the conduit and porous medium under 0.91 m (3.0 ft) and 1.82 m (6.0 ft) sea level rise conditions are quantitatively evaluated in this study (Fig. 13). Salinity at the submarine spring remains 35.0 PSU as same as the maximum seawater intrusion benchmark, but the head at the submarine spring increases to 0.91 m (3.0 ft) and 1.82 m (6.0 ft) as rising sea level, respectively. The width and shape of the mixing zone are similar to the simulation result in the maximum seawater intrusion benchmark. However, the mixing zone position moves landward in the conduit at almost 7.08 km from the shoreline when sea level rises 0.91 m (3.0 ft), which is 1.28 km further inland than the simulation with the present-day sea level. In the other extreme case of 1.82 m (6.0 ft) sea level rise, seawater intrudes additional 0.97 km further inland along the conduit than the case with 0.91 m (3.0 ft) sea level rise, or 2.25 km further inland than the simulation with present-day sea level. Compared with a homogeneous aquifer, seawater intrudes further landward through the conduit network in such a dual-permeability aquifer. The modeling of sea level rise confirm the concerns of severe seawater intrusion in the coastal region, also highlight the impacts on a karst aquifer with conduit system as the major pathway for seawater intrusion. In addition, sea level rise influence the regional flow field and hydrological conditions in a coastal aquifer. In Davis and Verdi (2014), increasing groundwater discharge at the inland Wakulla Spring in the WKP was observed associated with sea level rise in the past decades. The



735 relationship between spring discharge and sea level was quantitatively simulated by a
CFPv2 numerical model in Xu et al. (2015b). However, the changes of flow field and
hydrological conditions are not addressed and simulated in this study

(Insert Fig. 13 here)

740 **5.4 Extended low rainfall period**

The extents of seawater intrusion under scenarios of extended low rainfall periods
are presented in Fig. 14, although the elapsed time in simulation is not evaluated in the
sensitivity analysis. The simulated time period is extended to 14, 21 and 28 days, with the
conditions of salinity and sea level at the submarine spring as 35.0 PSU and 0.0 m,
745 respectively, as same as the maximum seawater intrusion benchmark.

(Insert Fig. 14 here)

During an extended low rainfall period, seawater intrudes through both the
conduit and the porous medium domains with time, since the 2.29 m (7.5 ft) equivalent
freshwater head at the submarine spring is higher than the inland freshwater boundary.
750 The mixing zone position also keeps moving landward slowly and persistently.
Compared with the maximum seawater intrusion benchmark with a stress period of 7-day
elapsed time in simulation, the mixing zone position after the 14-day simulation moves
additional 1.29 km landward in the conduit and the surrounding porous medium. In the
prediction of SEAWAT model, the mixing zone finally moves to 7.56 (7.89) km from the
755 shoreline after the 21 (28)-day extended low rainfall period. Above all, seawater keeps
intruding further inland through conduit network during an extended low rainfall period.



In such condition, the contamination of fresh groundwater resources in the aquifer becomes an environmental issue in coastal regions.

760 **6. Summary and Conclusion**

In this study, a 2D SEAWAT model is developed to evaluate the parameter sensitivities and quantitatively estimate seawater intrusion in a dual-permeability coastal karst aquifer with a conduit network. In the local sensitivities analysis, the composite scaled sensitivities (CSS) are calculated to assess the salinity and head simulations in the 765 conduit and the porous medium at specified parameter values. Salinity at the submarine spring (SC) is identified as the most important parameter to the simulations in both two domains, because the submarine spring is the major entrance of seawater intrusion into the conduit as pathway in the aquifer. The boundary conditions and hydrological characteristics of the conduit, including sea level at the submarine spring (H_SL), 770 hydraulic conductivity (HY_C) and effective porosity (PO_C) are important to the simulations in the conduit as well. On the other hand, the simulations in the porous medium also are sensitive to the boundary conditions (SC and H_SL) and hydrological characteristics of the conduit, such as specific storage and effective porosity (SS_C and PO_C), due to the interaction and exchange between the two domains. Sensitivity 775 analysis indicates that the observations and simulations in the conduit are especially important for understanding hydrogeological processes and modeling seawater intrusion in such a dual-permeability karst aquifer. In addition, the largest CSS values of parameter sensitivities can be found around the mixing zone position. The local sensitivity analysis in this study confirms the conclusions of sensitivity studies in a homogeneous aquifer in



780 Shoemaker (2004), also highlights the values of conduit network in modeling seawater intrusion in a coastal karst aquifer.

The global sensitivity analysis indicates that head simulation in the conduit is more sensitive to effective porosity (PO_C) and specific storage of the conduit (SS_C), instead of hydraulic conductivity. The conduit flow easily becomes non-laminar and 785 beyond the capability of Darcy equation in SEAWAT model, which assumes a linear relationship between specific discharge and head gradient. Therefore, the uncertainty of conduit permeability is difficult to be accurately evaluated by hydraulic conductivity in the continuum model. Different from the local sensitivity study, hydraulic conductivity of the porous medium (HY_P) has the largest mean of EEs with respect to head 790 simulation in the porous medium. Simulations are non-linear to parameter SC, which has the largest derivative in the specified evaluated location in the local sensitivity study., Dispersivity is no longer an important parameter for simulations in the conduit, which is different from Shoemaker (2004), because advection is dominated in the solution of saline water transport with turbulent flow in the conduit, as well as the relatively fast 795 seepage flow in the surrounding porous medium. In the salinity profile, the mixing is mostly due to numerical dispersion instead of the solution of dispersion equation, since Peclet number is extremely large and beyond the criteria of solving transport equation by finite difference method.

Seawater intrusion is quantitatively estimated with variations of salinity and sea 800 level at the submarine spring, which are identified as important parameters in sensitivity study. Seawater intrudes significantly further landward through the conduit, and flows into the surrounding porous medium via the exchange on the pipe wall. Salinity and head



boundary conditions of 35.0 PSU and 0.0 m, respectively, are set at the submarine spring in the case of the maximum seawater intrusion. The mixing zone position in the conduit 805 moves to 5.80 km from the shoreline with 1.13 km wide after a 7-day low rainfall period. Rainfall and regional recharges dilute the salinity at the submarine spring (SC), and significantly shift the mixing zone position seaward to 4.0 (4.5) km away from the shoreline with salinity of 10.0 (20.0) PSU. Compared with the benchmark, seawater intrudes additional 1.29 (2.25) km further landward along the conduit under 0.91 (1.82) 810 m sea level rise at the submarine spring (H_{SL}). In addition, the impacts of an extended low rainfall period on seawater intrusion through conduit network are also quantitatively assessed with longer elapsed time in simulation. The mixing zone position moves to 7.56 (7.89) km from the shoreline, after a 21 (28)-day low precipitation period.

In a summary, the conduit network is important as the major pathway for seawater 815 intrusion in the aquifer, and the submarine spring is the major entrance of seawater intrusion into the conduit. Some parameters, such as dispersivity and hydraulic conductivity in the conduit, have different sensitivities from the previous studies for a homogeneous aquifer. More attentions on the modeling and field observations in the karst features, including the subsurface conduit network, the submarine spring and karst 820 windows, are meaningful and important for calibrating the model and for understanding seawater intrusion in a coastal karst aquifer.

Competing interests

The authors declare that they have no conflict of interest.

825



References

Bear, J.: Seawater intrusion in coastal aquifers, Springer Science & Business Media, 1999.

Calvache, M., and Pulido-Bosch, A.: Effects of geology and human activity on the dynamics of salt-water intrusion in three coastal aquifers in southern Spain, *Environmental Geology*, 30, 215-223, 1997.

Custodio, E.: Salt-fresh water interrelationships under natural conditions, *Groundwater Problems in Coastal Areas*, UNESCO Studies and Reports in Hydrology, 45, 14-96, 1987.

835 Davis, J. H.: Hydraulic investigation and simulation of ground-water flow in the Upper Floridan aquifer of north central Florida and southwestern Georgia and delineation of contributing areas for selected City of Tallahassee, Florida, Water-Supply Wells, U.S. Geological Survey, Tallahassee, Florida, 55, 1996.

840 Davis, J. H., and Katz, B. G.: Hydrogeologic investigation, water chemistry analysis, and model delineation of contributing areas for City of Tallahassee public-supply wells, Tallahassee, Florida, Geological Survey (US)2328-0328, 2007.

Davis, J. H., Katz, B. G., and Griffin, D. W.: Nitrate-N movement in groundwater from the land application of treated municipal wastewater and other sources in the Wakulla Springs Springshed, Leon and Wakulla counties, Florida, 1966–2018, US Geol Surv Sci Invest Rep, 5099, 90, 2010.

845 Davis, J. H., and Verdi, R.: Groundwater Flow Cycling Between a Submarine Spring and an Inland Fresh Water Spring, *Groundwater*, 52, 705-716, 2014.

Diersch, H.: FEFLOW reference manual, Institute for Water Resources Planning and Systems Research Ltd, 278, 2002.

850 Essink, G., Van Baaren, E., and De Louw, P.: Effects of climate change on coastal groundwater systems: a modeling study in the Netherlands, *Water Resources Research*, 46, 2010.

Fleury, P., Bakalowicz, M., and de Marsily, G.: Submarine springs and coastal karst aquifers: a review, *Journal of Hydrology*, 339, 79-92, 2007.



855 Gallegos, J. J., Hu, B. X., and Davis, H.: Simulating flow in karst aquifers at laboratory and sub-regional scales using MODFLOW-CFP, *Hydrogeology Journal*, 21, 1749-1760, 2013.

Guo, W., and Langevin, C.: User's guide to SEWAT: a computer program for simulation of three-dimensional variable-density ground-water flow, *Water Resources Investigations Report*. United States Geological Survey, 2002.

Hill, M. C., and Tiedeman, C. R.: Effective groundwater model calibration: with analysis of data, sensitivities, predictions, and uncertainty, John Wiley & Sons, 2006.

Inouchi, K., Kishi, Y., and Kakinuma, T.: The motion of coastal groundwater in response to the tide, *Journal of Hydrology*, 115, 165-191, 1990.

865 IPCC: Contribution of Working Groups I, II and III to the Fourth Assessment Report of the Intergovernmental Panel on Climate Change, Geneva, Switzerland, 104 pp., 2007.

Kernagis, D. N., McKinlay, C., and Kincaid, T. R.: Dive Logistics of the Turner to Wakulla Cave Traverse, 2008.

Kincaid, T. R., and Werner, C. L.: Conduit Flow Paths and Conduit/Matrix Interactions

870 Defined by Quantitative Groundwater Tracing in the Floridan Aquifer, *Sinkholes and the Engineering and Environmental Impacts of Karst: Proceedings of the Eleventh Multidisciplinary Conference*, Am. Soc. of Civ. Eng. Geotech. Spec. Publ, 2008, 288-302,

Langevin, C. D., Shoemaker, W. B., and Guo, W.: MODFLOW-2000, the US Geological

875 Survey Modular Ground-Water Model--Documentation of the SEAWAT-2000 Version with the Variable-Density Flow Process (VDF) and the Integrated MT3DMS Transport Process (IMT), US Department of the Interior, US Geological Survey, 2003.

Martin, J. B., and Dean, R. W.: Exchange of water between conduits and matrix in the Floridan aquifer, *Chemical Geology*, 179, 145-165, 2001.

880 Martin, J. B., Gulley, J., and Spellman, P.: Tidal pumping of water between Bahamian blue holes, aquifers, and the ocean, *Journal of Hydrology*, 416, 28-38, 2012.

Moore, W. S., and Wilson, A. M.: Advective flow through the upper continental shelf driven by storms, buoyancy, and submarine groundwater discharge, *Earth and Planetary Science Letters*, 235, 564-576, 2005.



885 Morris, M. D.: Factorial sampling plans for preliminary computational experiments, Technometrics, 33, 161-174, 1991.

Poeter, E. P., and Hill, M. C.: Documentation of UCODE, a computer code for universal inverse modeling, DIANE Publishing, 1998.

Reimann, T., Liedl, R., Giese, M., Geyer, T., Maréchal, J.-C., Dörfliiger, N., Bauer, S., and Birk, S.: Addition and Enhancement of Flow and Transport processes to the MODFLOW-2005 Conduit Flow Process, 2013 NGWA Summit—The National and International Conference on Groundwater, 2013,

Reimann, T., Giese, M., Geyer, T., Liedl, R., Maréchal, J.-C., and Shoemaker, W. B.: Representation of water abstraction from a karst conduit with numerical discrete-continuum models, Hydrology and Earth System Sciences, 18, 227-241, 2014.

Saltelli, A., Tarantola, S., Campolongo, F., and Ratto, M.: Sensitivity analysis in practice: a guide to assessing scientific models, John Wiley & Sons, 2004.

Shoemaker, W. B.: Important observations and parameters for a salt water intrusion model, Ground Water, 42, 829-840, 2004.

900 Shoemaker, W. B., Kuniansky, E. L., Birk, S., Bauer, S., and Swain, E. D.: Documentation of a conduit flow process (CFP) for MODFLOW-2005, 2008.

Voss, C. I., and Provost, A. M.: SUTRA, US Geological Survey Water Resources Investigation Reports, 84-4369, 1984.

Voss, C. I., and Souza, W. R.: Variable density flow and solute transport simulation of regional aquifers containing a narrow freshwater - saltwater transition zone, Water Resources Research, 23, 1851-1866, 1987.

905 Werner, A. D., and Simmons, C. T.: Impact of sea - level rise on sea water intrusion in coastal aquifers, Groundwater, 47, 197-204, 2009.

Werner, A. D., Bakker, M., Post, V. E., Vandenbohede, A., Lu, C., Ataie-Ashtiani, B., Simmons, C. T., and Barry, D. A.: Seawater intrusion processes, investigation and management: recent advances and future challenges, Advances in Water Resources, 51, 3-26, 2013.

WHO: Guidelines for Drinking-water Quality, 104-108, 2011.



Wilson, A. M., Moore, W. S., Joye, S. B., Anderson, J. L., and Schutte, C. A.: Storm -
915 driven groundwater flow in a salt marsh, *Water Resources Research*, 47, 2011.

Xu, Z., Hu, B. X., Davis, H., and Cao, J.: Simulating long term nitrate-N contamination
processes in the Woodville Karst Plain using CFPv2 with UMT3D, *Journal of
Hydrology*, 524, 72-88, 2015a.

Xu, Z., Hu, B. X., Davis, H., and Kish, S.: Numerical study of groundwater flow cycling
920 controlled by seawater/freshwater interaction in a coastal karst aquifer through conduit
network using CFPv2, *Journal of contaminant hydrology*, 182, 131-145, 2015b.

Xu, Z., Bassett, S. W., Hu, B., and Dyer, S. B.: Long distance seawater intrusion through
a karst conduit network in the Woodville Karst Plain, Florida, *Scientific Reports*, 6, 2016.

Xu, Z., and Hu, B. X.: Development of a discrete - continuum VDFST - CFP numerical
925 model for simulating seawater intrusion to a coastal karst aquifer with a conduit system,
Water Resources Research, 53, 688-711, 10.1002/2016WR018758., 2017.



Table 1. The symbols and definitions of parameters used in this study, the specified evaluated values in local sensitivity study and evaluation ranges (the lower and upper constraints) of each parameter in global sensitivity analysis.

Parameter	Definitions	Lower	Upper	Evaluated value	Unit
HY_P	Hydraulic conductivity (porous medium)	1.524	4.572	2.286	meter/day ($\times 10^3$)
HY_C	Hydraulic conductivity (conduit)	3.048	9.144	6.096	meter/day ($\times 10^5$)
SS_P	Specific storage (porous medium)	4.00	6.00	5.00	dimensionless ($\times 10^{-7}$)
SS_C	Specific storage (conduit)	0.03	0.07	0.05	dimensionless
RCH	Recharge rate on the surface	0.00	0.03	0.01	meter/day
H_SL	Sea level at the submarine spring	-0.305	0.914	0.305	meter
PO_P	Porosity (porous medium)	0.001	0.005	0.003	dimensionless
PO_C	Porosity (conduit)	0.200	0.400	0.300	dimensionless
SC	Salinity at the submarine spring	0.0	35.0	35.0	PSU
DISP_P	Longitudinal dispersivity (porous medium)	6.10	12.20	10.00	meter
DISP_C	Longitudinal dispersivity (conduit)	0.15	0.60	0.30	meter

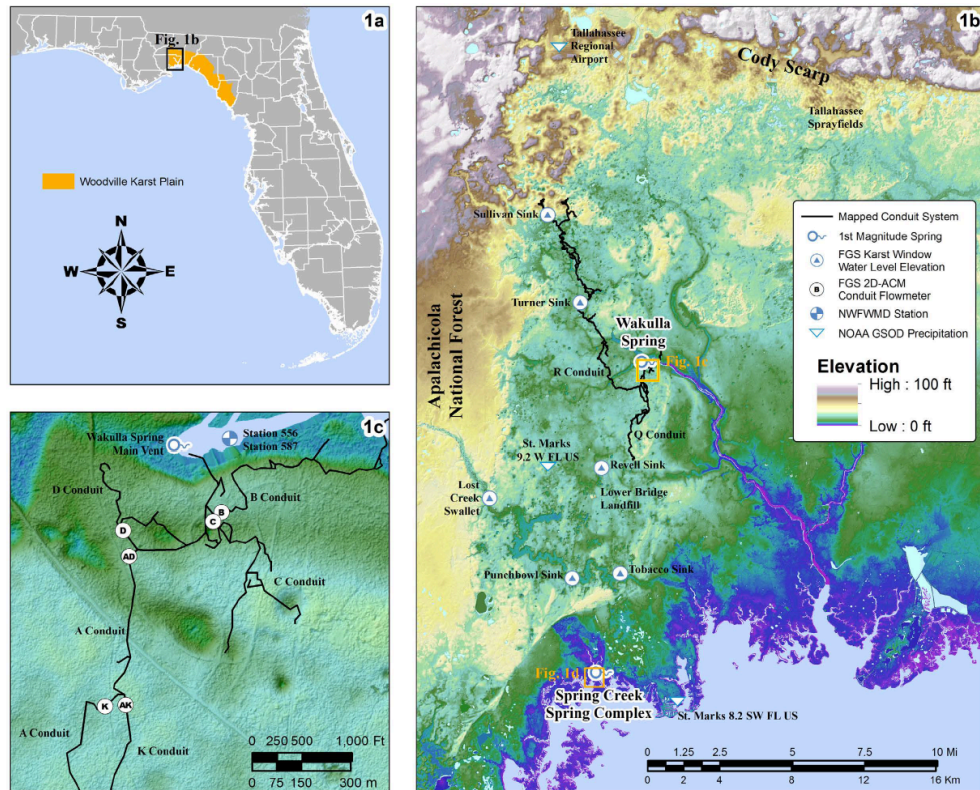


Figure 1. a) Locations of the Woodville Karst Plain (WKP) and the study site; b) The map of the Woodville Karst Plain showing the locations of features of note with the study; c) The detail of cave system near Wakulla Springs. Modified from Xu et al., (2016).

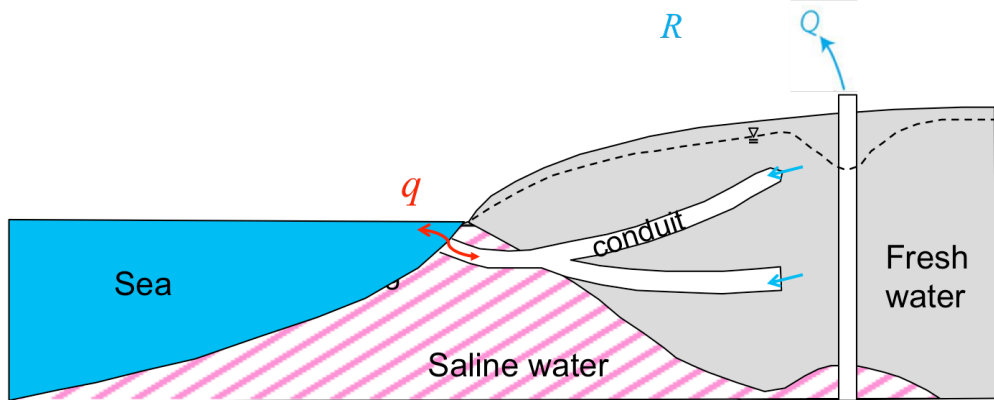
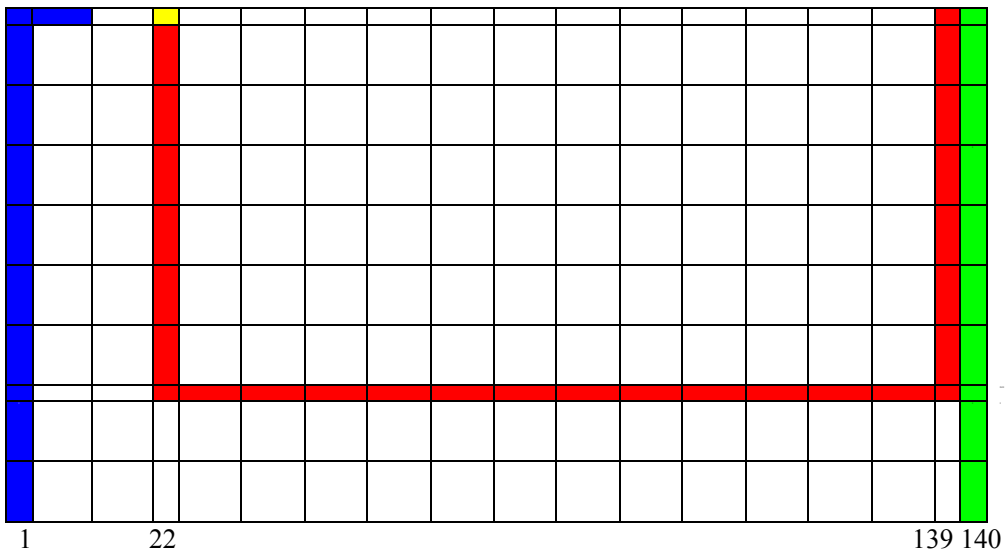


Figure 2. Schematic figure of a coastal karst aquifer with conduit networks and a submarine spring opening to the sea in a cross section. Flow direction q would be seaward when sea level drops, pumping rate Q is low and precipitation recharge R is large; however, reversal flow occurs when sea level rises, pumping rate Q is high or precipitation recharge R is small.



Explanations:

- Constant head and constant concentration of the submarine spring and outlet of karst conduit system, however, various in different cases of numerical models
- Sea-edge boundary: constant head (0.0 ft in normal sea level case) and constant concentration (35 PSU)
- Inland boundary: constant head (5.0 ft) and constant concentration (0 PSU)
- Conduit: high hydraulic conductivity, porosity and specific storage
- Porous medium: low hydraulic conductivity, porosity and specific storage

Figure 3. Schematic figure of finite difference grid discretization and boundary conditions applied in the SEAWAT model. Every cell represents 10 horizontal cells and 4 vertical cells, except the boundary and conduit layer in color with smaller width. The submarine spring is located at column #22, layer #1, and the inland spring is located at column #139, layer #1. The conduit system starts from the top of column #22, descends downward to layer #29, horizontally extends to column #139, and then rises upward to the top through column #139.

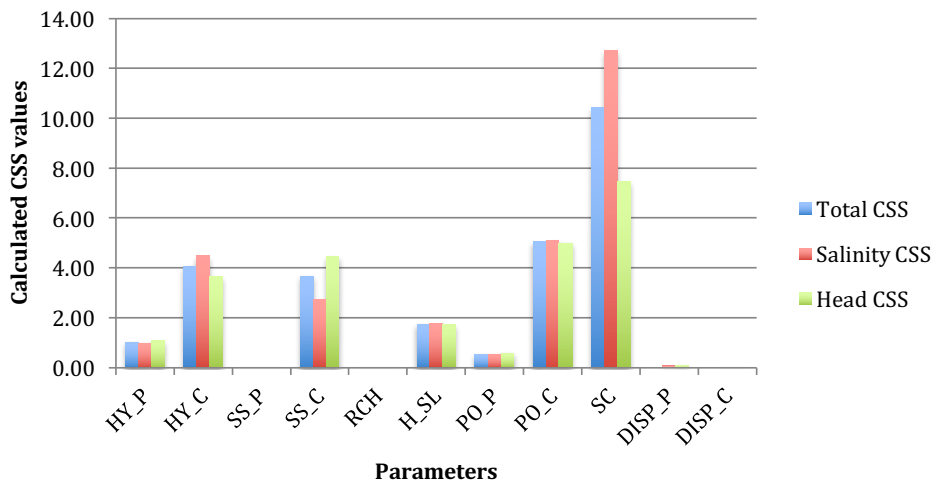


Figure 4. The CSSs (Composite Scaled Sensitivities) of all parameters with respect to simulations in the conduit (layer #29) in the local sensitivity analysis.

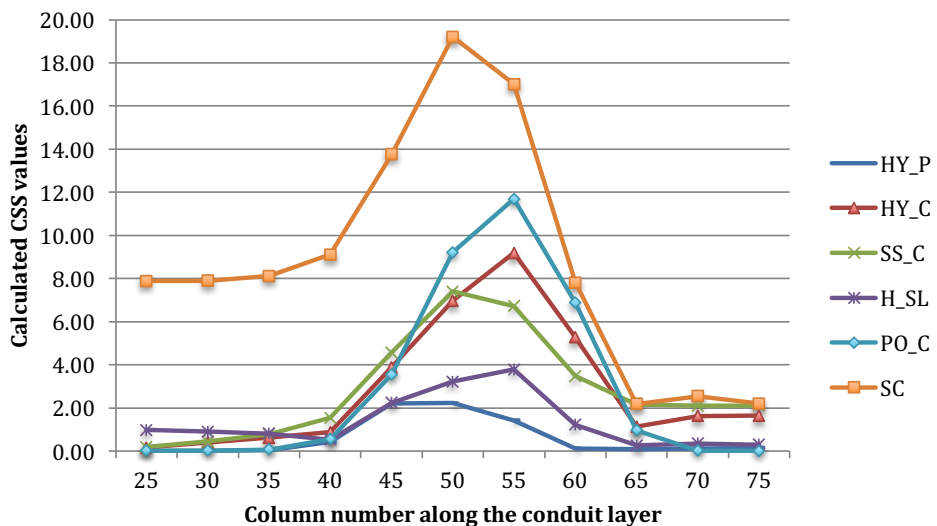


Figure 5. The CSSs (Composite Scaled Sensitivities) of selected parameters at different locations along the conduit layer (from column #25 to column #75) in the local sensitivity analysis.

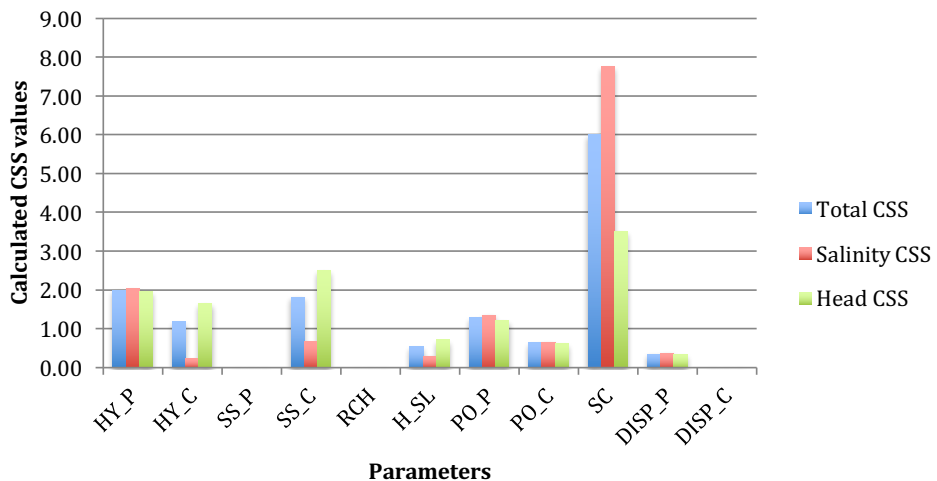


Figure 6. The CSSs (Composite Scaled Sensitivities) of all parameters with respect to simulations in the porous medium (layer #24) in the local sensitivity analysis.

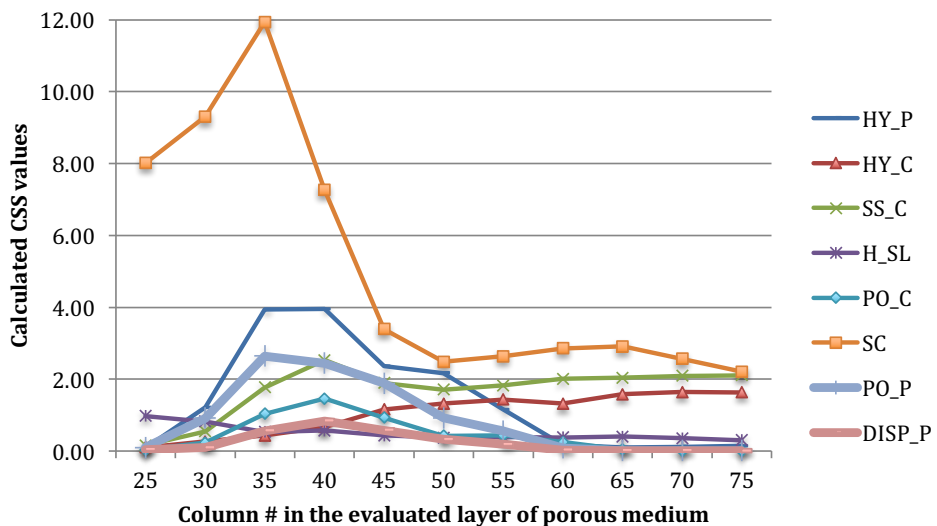


Figure 7. The CSSs (Composite Scaled Sensitivities) at different locations in the porous medium (from column #25 to column #75 at layer # 24) in the local sensitivity analysis.

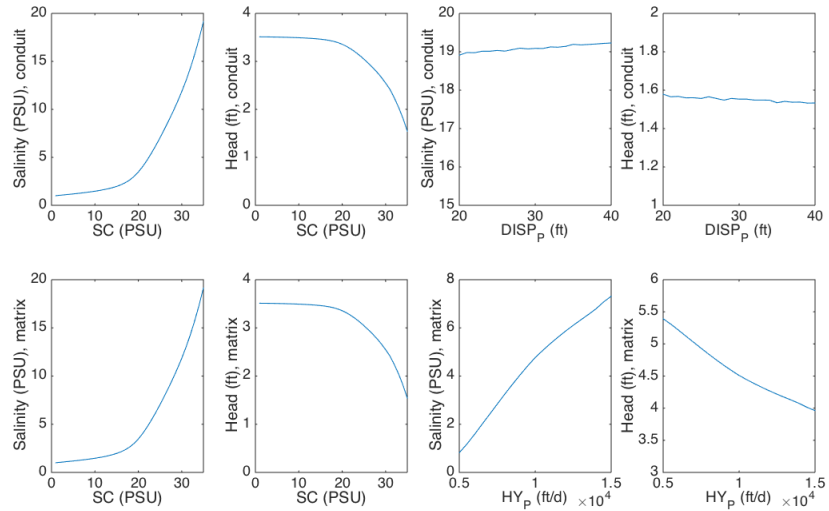


Figure 8. The non-linear relationship between head and salinity simulations with respect to parameters SC, DISP_P and HY_P. (Note that the scale for each plot is different).

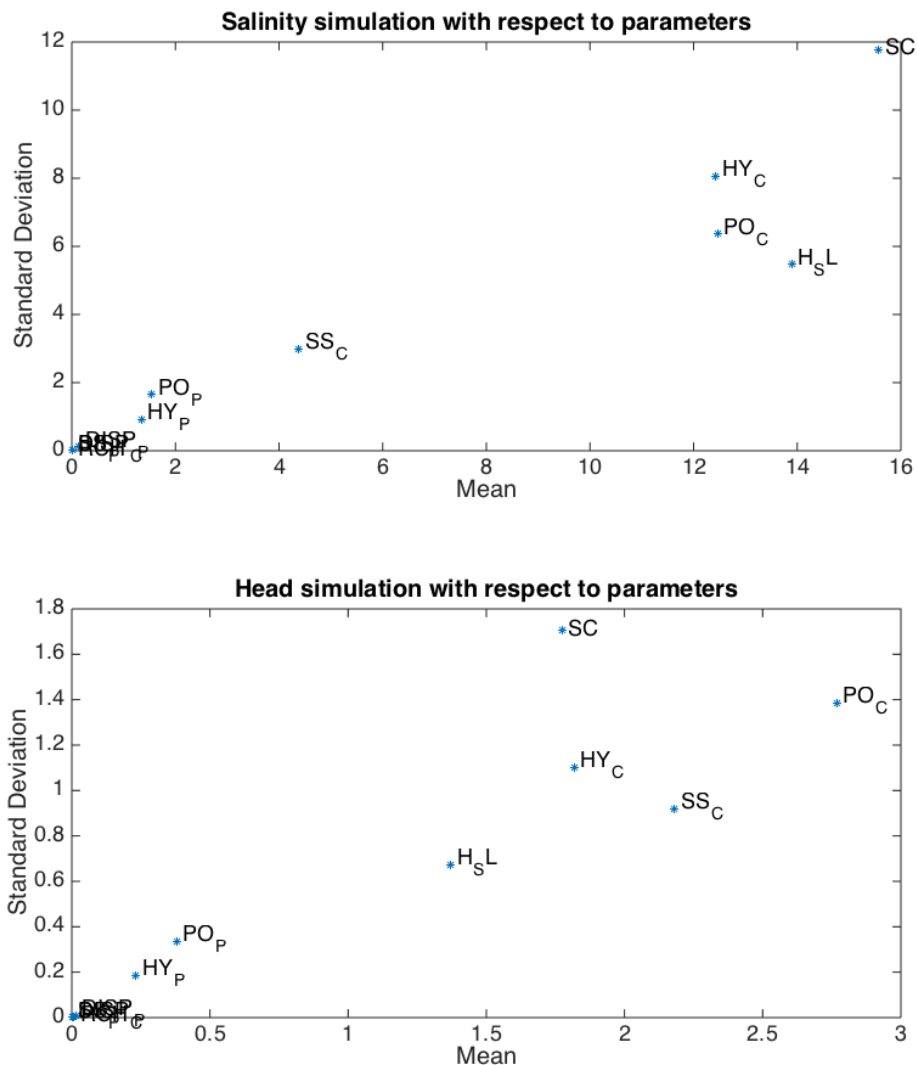


Figure 9. Mean and standard deviation of the EEs (elementary effects) of parameters with respect to simulations in the conduit (column #50, layer #29) by the trajectory sampling Morris method in the global sensitivity analysis: a) salinity simulation (top); b) head simulation (bottom).

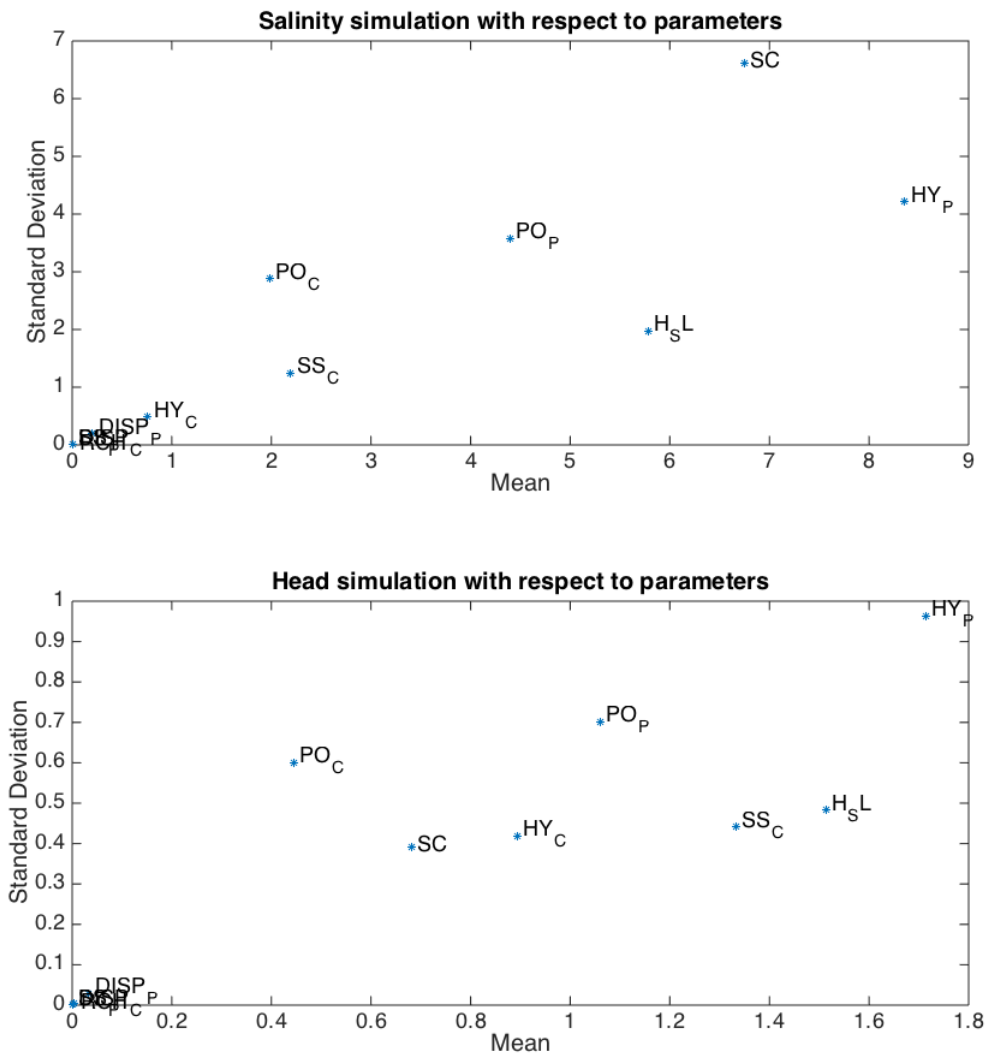


Figure 10. Mean and standard deviation of the EEs (elementary effects) of parameters with respect to simulations in the porous medium (column #35, layer #24) by trajectory sampling Morris method in the global sensitivity analysis: a) salinity simulation (top); b) head simulation (bottom).

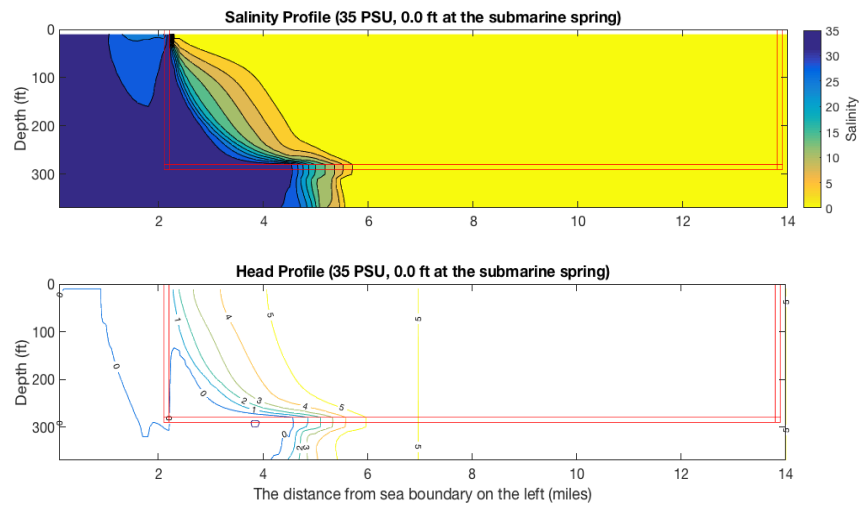


Figure 11. Salinity (top) and head (bottom) simulations of the maximum seawater intrusion case (35 PSU, 0.0 ft at the submarine spring).

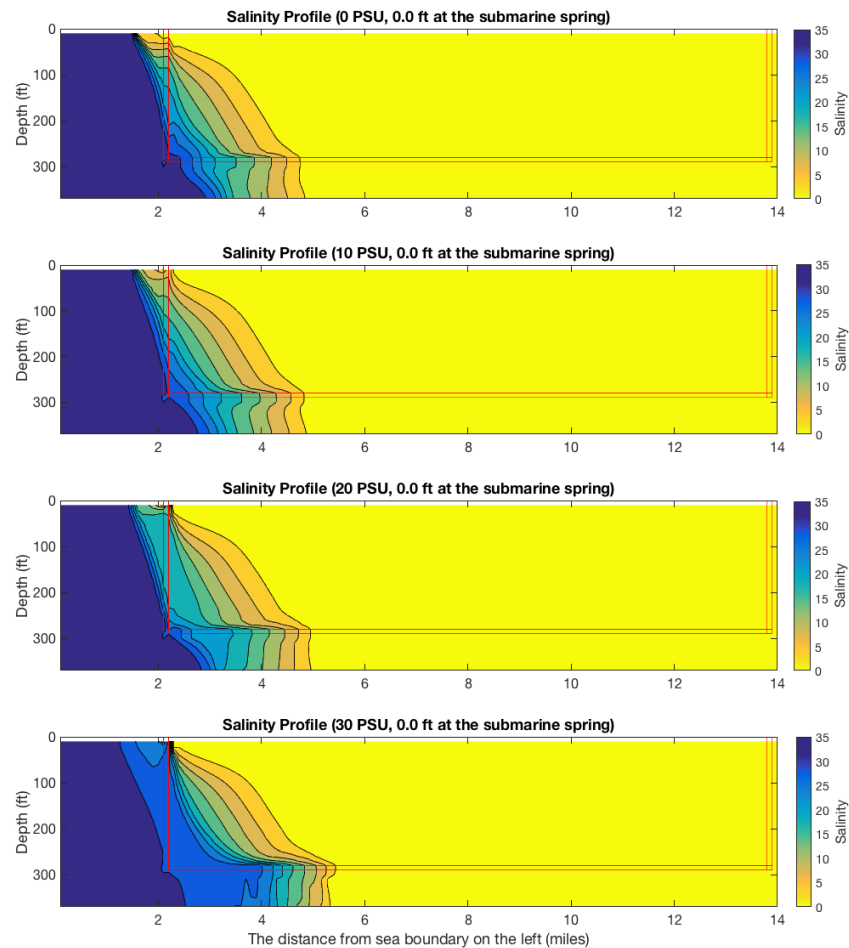


Figure 12. Salinity simulation of seawater intrusion with various salinity at the submarine spring, indicating different rainfall recharge and freshwater discharge conditions: A) 0.0 PSU, 0.0 ft at the submarine spring; B) 10.0 PSU, 0.0 ft at the submarine spring; C) 20.0 PSU, 0.0 ft at the submarine spring; D) 30.0 PSU, 0.0 ft at the submarine spring (from top to bottom).

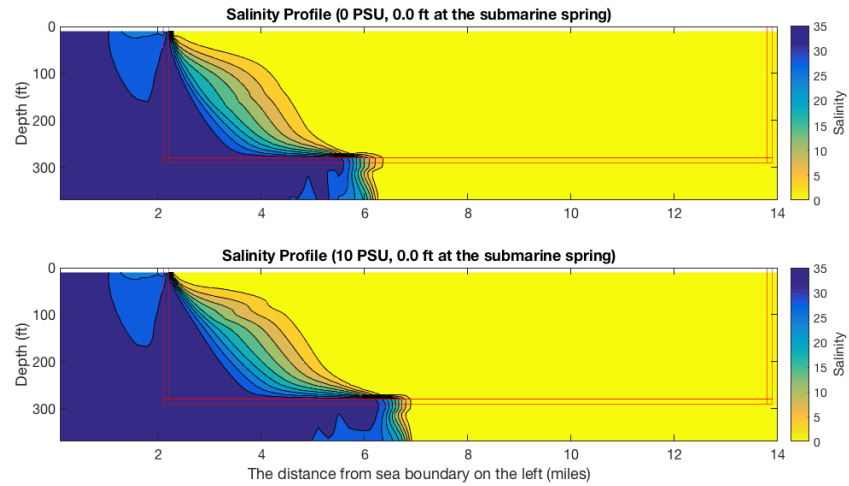


Figure 13. Salinity simulation of seawater intrusion with various sea level conditions: A) 35.0 PSU, 3.0 ft at the submarine spring; B) 35.0 PSU, 6.0 ft at the submarine spring (from top to bottom).

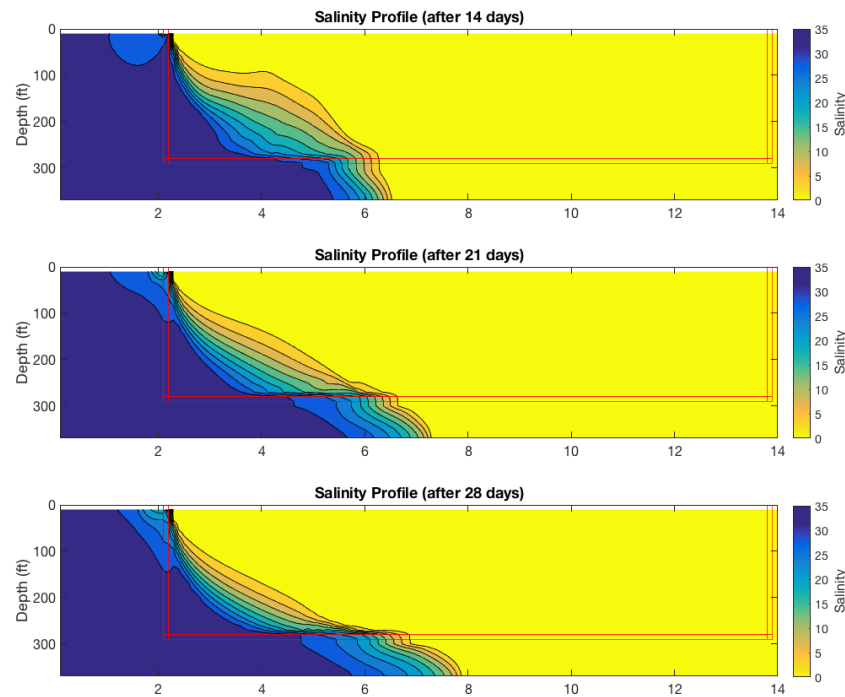


Figure 14. Salinity simulation of the maximum seawater intrusion case (35 PSU, 0.0 ft at the submarine spring) with extend simulation time during a low rainfall period: A) 14-day simulation period; B) 21-day simulation period; C) 28-day simulation period (from top to bottom).